MOBILE MAPPING SYSTEMS – STATE OF THE ART AND FUTURE TRENDS

Dr. Klaus Peter Schwarz and Dr. Naser El-Sheimy

Invited Paper
Department of Geomatics Engineering, University of Calgary
2500 University Drive NW, Calgary, Alberta, T2N 1N4 Canada – kpschwar@telusplanet.net and naser@geomatics.ucalgary.ca

TS SS 3 – Mobile Multi-sensor Systems

KEY WORDS: Mobile Mapping, Direct Georeferencing, GPS/INS, Real-time mapping

ABSTRACT:

Digital mobile mapping, the methodology that integrates digital imaging with direct geo-referencing, has developed rapidly over the past fifteen years. What used to be a topic of academic study has become a commercially viable industry. In this paper the major steps in this development are traced and the current state of the art is reviewed. This is done by looking at developments in four specific areas: digital imaging, direct geo-referencing, mathematical modeling, filtering and smoothing. The paper concludes with a look into the future and the discussion of some ongoing research at the University of Calgary.

1. INTRODUCTION

The idea of mobile mapping, i.e. mapping from moving vehicles, has been around for at least as long as photogrammetry has been practiced. The early development of mobile mapping systems (MMS) was, however restricted to applications that permitted the determination of the elements of exterior orientation from existing ground control. About fifteen years ago, advances in satellite and inertial technology made it possible to think about mobile mapping in a different way. Instead of using ground control as reference for orienting the images in space, trajectory and attitude of the imager platform could now be determined directly. This has made mapping independent of pre-established ground control. Hand in hand with this development went the change from analog to digital imaging techniques – a change that has considerably accelerated over the past few years. Integrating the concepts of kinematic trajectory determination and digital imaging resulted in multi-sensor systems capable of acquiring, storing, and processing geo-referenced digital data, thus providing a complete solution of the mapping problem with data from only one platform. Systems that use geo-referencing and digital imaging as integral parts will in the following be considered as mobile mapping systems, independent of their area of application.

Combining the advances in digital imaging and direct geo-referencing has not only increased the efficiency of mobile mapping considerably, but has also resulted in greater flexibility and lower cost. In addition, it has integrated two branches of our discipline that for too long have gone their separate ways – geodesy and remote sensing/photogrammetry. In this paper, recent developments in mobile mapping will be reviewed and some emerging applications and future trends will be discussed.

2. DIGITAL IMAGING

In digital imaging film-based optical sensors are replaced by fully digital electro-optical or active electronic sensors, often with multi-spectral capabilities. These sensors are conveniently categorized as frame-based, as in the case of digital cameras, or as line scanners, as in case of multispectral scanners (casi, MEIS), Lidar systems, or the radar-based InSar systems. The development of MMS is tied to the development of digital sensor technology. This is most evident in the case of frame-based digital cameras. Digital imaging with these sensors is closest in concept to airborne photogrammetric mapping. Their first use, however, was in land-vehicle applications, not in airborne applications. The obvious reason is that in land-vehicle MMS the camera-to-object distances are much smaller than in standard airborne applications. The poor resolution of CCD chips meant that they could not be used in aerial applications without a major loss in accuracy. Indeed, the resolution of CCD chips has only recently improved to the level that they can be used in airborne mapping systems, albeit without yet achieving the accuracy of film-based sensors. The use of digital cameras is advantageous because they eliminate the requirement to scan photographs. Consequently they substantially reduce the period from raw data collection to extracted data dissemination. Digital sensors also simplify automatic point and feature extraction, and allow for more flexible data storage possibilities – for example, the images can be stored in Multi-Media GIS [Novak, 1993].

Although many of the current aerial photogrammetric systems are film-based, it is expected that the use of film and conventional stereo plotters will soon be replaced by fully digital cameras and digital photogrammtric workstations. Today's digital cameras have some inherent limitations and don't produce the sameresolution as film-based cameras. A standard aerial photo with 40 lp/mm corresponds to 18400 x 18400 pixel. Currently no CCD-chips with such a resolution are available. However, the rapid pace of digital camera evolution renders the new medium a force to be reckoned with. CCD-cameras with up to 4000 x 4000 pixels, such as the Applanix DSS system (Mostafa, 2004), are already used in commercial applications. Other manufacturers are developing systems that will replace film-based cameras, possibly within the next year.

Other commercial developments are ongoing in the area of line scanners and include the Leica Geosystems Airborne Digital Sensor (ADS40TM) and the ZI Digital Mapping Camera (DMCTM). The ADS40TM which has been developed in co-operation with the DLR (Deutsches Zentrum für Luft- und

Raumfahrt – the German Aerospace Centre) is a three-line pushbroom scanner with 28° forward fore and 14°aft viewing angles from the nadir. With this design each object point is imaged 3 times with a stereo angle of up to 42°. Each panchromatic view direction includes 2 CCD-lines, each with 12000 pixels in staggered arrangement, leading to 24 000 pixels, covering a swath of 3.75km from a flying altitude of 3000m with a 15cm ground pixel size. The DMCTM has a different design; it integrates 4 digital panchromatic cameras (and 4 multispectral 3k x 2k cameras) with CCD of 4Kx7K resolution, resulting in images with 8k by14k resolution. With a pixel size of 12µm x 12µm and a focal length of 120mm, the camera has a 43.1° by 75.4° field of view. A bundle block adjustment of a small block with crossing flight directions with an image scale 1:12 800 (flying height 1500m) resulted in a sigma0 of 2µm (1/6 pixel). At independent check points standard deviations of $\sigma_x = \sigma_y$ =+/-4cm corresponding to 3.3µm in the image (1/4 pixel) and σ_z =+/-10cm corresponding to 2.7µm x-parallax were achieved (Doerstel et al 2002). Such accuracy is far beyond what is achievable with a film-based camera. It should be noted that although digital frame cameras do currently not reach the accuracy of film-based sensors, other digital imaging techniques surpass them by a considerable margin.

Another important development in digital imaging is the development of airborne hyperspectral imaging sensors. These sensors are used to map different bands of the visible and invisible spectrum. Typically they are pushbroom scanners and can produce more than 100 different bands or channels. The combination of specific bands produces a unique signature for each material in the scene. These signatures are used to classify and identify the materials present at each location. It is therefore an excellent tool for environmental assessments, mineral mapping and exploration, vegetation communities and species, health studies, and general land management studies. This imagery is especially powerful when combined with LIDAR points or the LIDAR generated surface. For example the extraction of forest canopy heights can be accomplished using a combination of hyperspectral classification and LIDAR based multiple return analysis techniques.

Among the new technologies, Airborne IFSAR (Interferometric Synthetic Aperture Radar) mapping is attracting much attention in the geo-spatial community. This attention is due to the flexibility of system deployment, near weather-independent operation, cloud penetrating capability, versatile map products, and quick turn-around time. As a result, high-resolution airborne IFSAR systems are providing data to applications traditionally supported by conventional Photogrammetric technology. The three main products are, Digital Elevation Models (DEMs), digital Orthorectified Radar Images (ORRIs), and Topographic Line Maps (TLMs).

3. DEVELOPMENT OF GEO-REFERENCING TECHNOLOGY

Direct geo-referencing is the determination of time-variable position and orientation parameters for a mobile digital imager. The most common technologies used for this purpose today are satellite positioning by GPS and inertial navigation using an Inertial Measuring Unit (IMU). Although each technology can in principle determine both position and orientation, they are usually integrated in such a way that the GPS receiver is the main position sensor, while the IMU is the main orientation sensor. The orientation accuracy of an IMU is largely determined by the gyro drift rates, typically described by a bias (constant drift rate), the short tem bias stability, and the angle random walk. Typically, four classes of gyros are distinguished according to their constant drift rate, namely:

1. strategic gyros (0.0005-0.0010 deg/h or degree per month)
2. navigation-grade gyros (0.002-0.01 deg/h or degree per week)
3. tactical gyros (1-10 deg/h or degree per hour)
4. low-accuracy gyros (100-10 000 deg/h or degree per second)

Only the last three classes will be discussed in the following.

Operational testing of direct geo-referencing started in the early nineties, see for instance Cannon and Schwarz (1990) for airborne applications, and Lapucha et al (1990) for land-vehicle applications. These early experiments were done by integrating differential GPS with a navigation-grade IMU (accelerometer bias: 2-3 10-4ms-2, gyro bias: 0.003 deg/h) and by including the derived coordinates and attitude (pitch, roll, and azimuth) into a photogrammetric block adjustment. Although GPS was not fully operational at that time, results obtained by using GPS in differential kinematic mode were promising enough to pursue this development. As GPS became fully operational the INS/DGPS geo-referencing system was integrated with a number of different imaging sensors. Among them were the Casi sensor manufactured by Itres Research Ltd., see Cosandier et al (1993); the MEIS of the Canada Centre for Remote Sensing, see ; and a set of CCD cameras, see El-Sheimy and Schwarz (1993). Thus, by the end of 1993 experimental systems for mobile mapping existed for both airborne and land vehicles. A more detailed overview of the state of the art at that time is given in Schwarz et al (1993). The evolution of the geo-referencing technology during the past decade was due to the ongoing refinement and miniaturization of GPS-receiver hardware and the use of low and medium cost IMU's that became available in the mid-nineties. Only the latter development will be briefly discussed here.

The inertial systems used in INS/GPS integration in the early nineties were predominantly navigation-grade systems, typically strapdown systems of the ring-laser type. When integrated with DGPS, they provided position and attitude accuracies sufficient for all accuracy classes envisaged at that time. These systems came, however, with a considerable price tag (about US $ 130 000 at that time). With the rapidly falling cost of GPS-receiver technology, the INS became the most expensive component of the geo-referencing system. Since navigation-grade accuracy was not required for the bulk of the low and medium accuracy applications, the emergence of low-cost IMU in the mid-nineties provided a solution to this problem. These systems came as an assembly of solid state inertial sensors with analog read-outs and a post-compensation accuracy of about 10 deg/h for gyro drifts and about 10-2 ms-2 for accelerometer biases. Prices ranged between US$ 10 000 and 20 000 and the user had to add the A/D portion and the navigation software. Systems of this kind were obviously not suited as stand-alone navigation systems because of their rapid position error accumulation. However, when provided with high-rate position and velocity updates from differential GPS (1s pseudo-range solutions), the error growth could be kept in bounds and the position and attitude results from the integrated solution were suitable for low and medium accuracy applications.; for details on system design and performance, see Bäumker and Matissek (1992),

Lipman (1992), Bader (1993), and Knight et al (1993) among others.

With the rapid improvement of fibre optic gyro performance, the sensor accuracy of a number of these systems has improved by about an order of magnitude (1 deg/h and 10-1ms-2) in the past five years. Typical cost are about US$ 30 000. Beside the increased accuracy, these systems are more user friendly and offer a number of interesting options. When integrated with a DGPS phase solution the resulting position and attitude are close to what is required for the high-accuracy class of applications. When aiming at highest possible accuracy these systems are usually equipped with a dual-antenna GPS, aligned with the forward direction of the vehicle. This arrangement provides regular azimuth updates to the integrated solution and bounds the azimuth drift. This is of particular importance for flights flown at constant velocity along straight lines, as is the case for photogrammetric blocks. Commercialization of the mobile mapping system concept for all application areas has been done by the Applanix Corporation (now a subsidiary of Trimble – www.applanix.com). In general, the position and orientation accuracy achieved with these systems is sufficient for all but the most stringent accuracy requirements; for details see chapter 7)

During the past few years a new technology has rapidly changed manufacturing processes in engineering, specifically in sensor design and telecommunications. It is called MEMS technology for its products, which are Micro Electronic Mechanical Systems (MEMS). Accelerometers and gyros are among the early products manufactured in this way. They are micro-machined and, when produced in large quantities, will be extremely inexpensive. Current prices per sensor range from US$ 20 – 150, depending on accuracy, but predictions are that they will get into the range of dimes rather than dollars. T The inertial sensors produced until recently by MEMS were for the mass market and were of poor quality when compared to navigation-grade inertial sensors. Gyros had constant drift rates of thousands of degrees per hour. However, results recently presented at IEEE PLANS 2004 indicate that companies are actively working on MEMS-based tactical gyros, see for instance Hanse (2004) and Geen (2004). Considering that the production processes for MEMS inertial sensors are relatively new and that the improvement potential is considerable, can it be expected that at some point in the future the accuracy of these sensors may be sufficient to support navigation-type applications? At this point it is not possible to answer this question in an unequivocal way. However, two arguments will be given, one in favor, the other against. They may be helpful for forming an opinion.

The argument against is based on some interesting empirical results that the authors received by courtesy of Dr. Robert J. Smith at the Honeywell Technology Center. They have been partly reproduced in Figure 1. Gyro performance (measured by long-term bias stability) is plotted vs. the nominal size of the gyro on a log-log scale. It should be noted that the figure is not based on a comprehensive market analysis, but is an in-house study conducted by Dr. Smith. This is the reason why only Honeywell gyros are shown. The gyros represented in this figure vary in terms of size (between 120 mm and 4 mm) and principle used (RLG, ESG, HRG, FOG, 2DF rotor, QRS). All, except one, are production-type systems. Each gyro is represented by an ellipse showing the performance range in horizontal direction and the variability in size in vertical direction. It is remarkable that the line N=4 gives such a close fit to most gyros presented in the chart. This indicates that gyro accuracy, independent of the principle used, is determined by the size of the sensor. The gyros above the line fit are typically not pressing the state of the art, because of other considerations (cost, lifetime). For the one gyro below the line, the H-ESG, which seems to outperform the general trend, only bias stability values in a benign temperature environment were available. It might therefore not be directly comparable to the other performance values which cover a wide range of production environments.

Excluding these special cases, the N=4 line can be considered as an empirical law for gyro performance which is independent of the principle used to build the gyro. This means that it can be used as a predictor for gyro performance in cases where the size of the gyro is given by other considerations. When applying this principle to the MEMS gyro environment it would mean that a gyro with a nominal size of 2mm would perform at the 10 000 deg/h level, while a tactical grade gyro with a performance of 1-10 deg/h should have a minimal size of about 20 mm. Chip size will essentially limit the accuracy of the IMU-on-a-chip. Similarly, the likelihood that MEMS-based gyroscopes will reach navigation-grade performance is tied to the nominal size of the gyro which has to be about 6 cm to achieve the requirements.

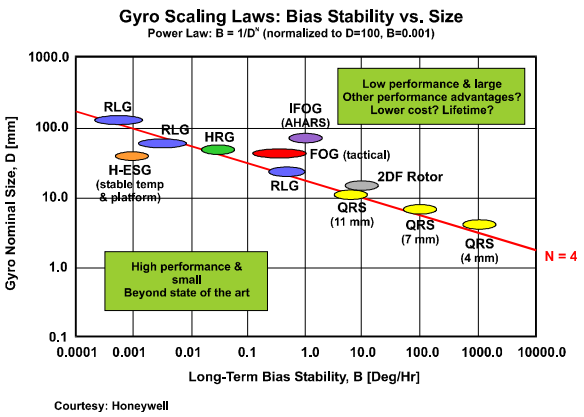

Figure 1: Bias Stability vs. Nominal Size for Mature Gyro Technology.

The argument in favor of MEMS gyro usage for navigation-type applications is based on publications recently presented at the IEEE PLANS 2004 and results obtained by the Mobile Multi-Sensor Research Group at the University of Calgary, Canada. The latter were obtained in a land-vehicle test using a MEMS-based IMU developed by employing off-the-shelve MEMS sensors with an average cost 20$ per sensor (see Figure 2). The test also included the Honeywell CIMU, a navigation grade inertial navigation system, and DGPS. Both DGPS and CIMU trajectories were available throughout the whole test and were used as an accurate reference for the MEMS IMU results. Inertial measurements of MEMS sensors were integrated with the single point positioning GPS output (accurate to 10 -30 m) and processed through the INS Tool Box (Shin and El-Sheimy, 2003) Kalman filter software. GPS signals from a minimum of seven satellites were available throughout the test. In order to assess the performance of the integrated system, GPS outages of 30 seconds were simulated, by removing GPS data, along various portions of the test trajectory. Figure 3 shows the

positional error of the integrated MEMS IMU and GPS during the simulated GPS outages. The figure clearly indicates that the IMU stand-alone results during the GPS outages are within 5-10 m (RMS). This accuracy meets the general requirements for car navigation. A possible explanation for this surprising performance is the bias calibration procedure applied to the IMU. It successfully eliminated the long-term gyro bias. Since the short-term bias is much smaller, of the order of 50 deg/h, short outages like the ones simulated here can be bridged quite well. These results are confirmed by those in Hanse (2004) and Geen (2004).

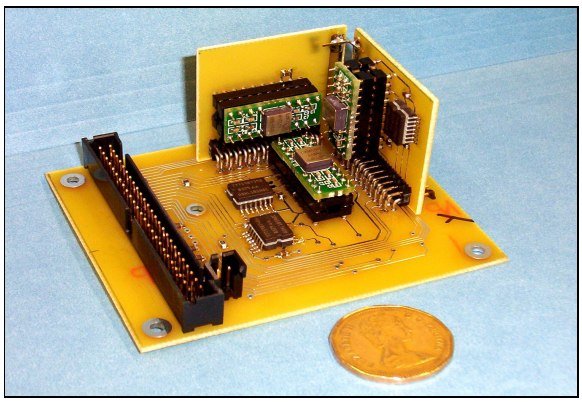

Figure 2: University of Calgary MEMS-based IMU (without case)

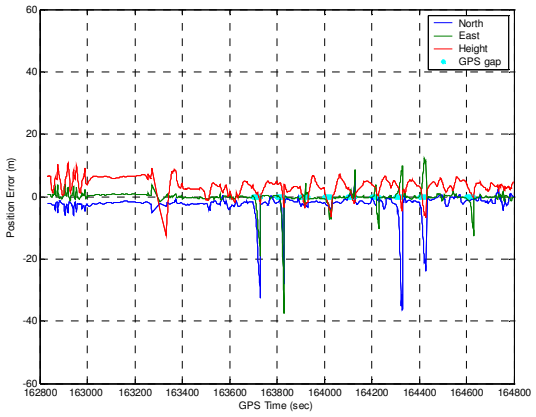

Figure 3: Positional Drift during GPS blockage

4. MATHEMATICAL MODELING

The formulation of the direct geo-referencing formula is rather straight-forward, for details see for instance Schwarz (2000). The standard implementation of this formula will, however, cause difficulties when low-accuracy gyros are used. The modifications necessary in this case will be discussed in this chapter. Figure 4 depicts airborne mobile mapping using a digital frame camera. The mathematical model is given in equation (1) and will be used as the standard model in the following discussion. The terms in the equation are listed in Table 1.

$$r_i^m = r_{nav}^m(t) + R_b^m(t)[s_i \bullet R_c^b \bullet r^c + a_{INS}^c - a_{INS}^{GPS}] \qquad [1]$$

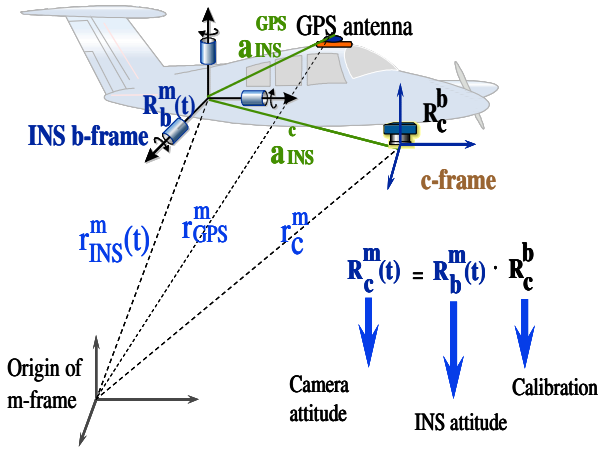

Figure 4: Principle of Airborne Geo-referencing

Variable	Obtained from
r_i^m	is the coordinate vector of point (i) in the mapping frame (m-frame) **Unknown** (3)
$r_{nav}^m(t)$	is the interpolated coordinate vector of the navigation sensors (INS/GPS) in the m-frame
S^i	is a scale factor, determined by stereo techniques, laser scanners or DTM
$R_b^m(t)$	is the interpolated rotation matrix between the navigation sensor body frame (b-frame) and the m-frame
(t)	is the time of exposure, i.e. the time of capturing the images, determined by synchronization
R_c^b	is the differential rotation between the C-frame and the b-frame, determined by calibration
r^c	is the coordinate vector of the point in the C-frame (i.e. image coordinate),
r_{INS}^c	vector between IMU center and camera principal point, determined by calibration
r_{INS}^{GPS}	vector between IMU center and GPS antenna center, determined by calibration

Table 1: Elements of the Georeferencing Formula

Implementation of this formula requires inertial and GPS measurements for the determination of the two time-dependent terms on the right-hand side of equation (1), as well as image coordinate measurements, in the c-frame, for the determination of the object point coordinate vector r^c. The c-frame has its origin in the perspective centre of the camera, its z-axis is defined by the vector between the perspective centre and the principal point of the photograph, and its (x,y)-axes are defined in the plane of the photograph and are measured with respect to the principal point. The corresponding image vector is therefore of the form:

$$\mathbf{r^c} = \begin{pmatrix} x - x_p \\ y - y_p \\ -f \end{pmatrix}, \text{ where}$$

(x_p, y_p) are the principal point coordinates
f is the camera focal length

If instead of a frame camera, either a pushbroom scanner or a Lidar system are modeled, the only change necessary is in the term r^c. It will have the form for :

- A pushbroom scanner = $\begin{pmatrix} 0 \\ y - y_p \\ -f \end{pmatrix}$
- A LIDAR scanner = $\begin{pmatrix} -d \cdot \sin\alpha \\ 0 \\ -d \cdot \cos\alpha \end{pmatrix}$ where,

d Raw laser range (distance) in laser frame

α Scanner angle from nadir along y-axis of laser frame, see Figure 5

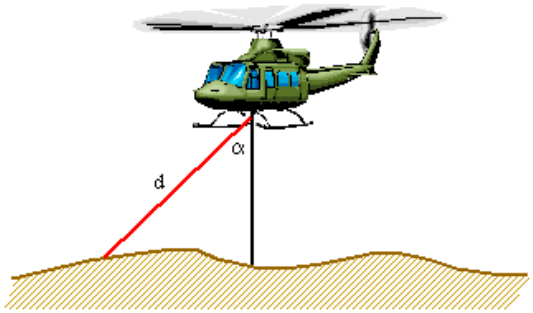

Figure 5: LIDAR Scanner Angle and Distance Measurement

In addition, the misalignment matrix R_c^b and the offset vectors r_{INS}^c and r_{INS}^{GPS} have to be determined by calibration. A detailed discussion of implementation aspects can be found in El-Sheimy (1996) for land-vehicle applications and in Mostafa and Schwarz (2000) for airborne applications.

Using Newton's second law of motion in a rotating coordinate frame, the inertial sensor measurements - specific force $\mathbf{f}^b$ and angular velocity $\boldsymbol{\omega}_{ib}^b$, measured in the b-frame – can be transformed into an Earth-fixed frame, say the Conventional Terrestrial Coordinate Frame(e). The resulting system of differential equations is of the form

$$\begin{pmatrix} \dot{\mathbf{r}}^e \\ \dot{\mathbf{v}}^e \\ \dot{\mathbf{R}}_b^e \end{pmatrix} = \begin{pmatrix} \mathbf{v}^e \\ \mathbf{R}_b^e \mathbf{f}^b - 2\boldsymbol{\Omega}_{ie}^e \mathbf{v}^e + \mathbf{g}^e \\ \mathbf{R}_b^e (\boldsymbol{\Omega}_{ib}^b - \boldsymbol{\Omega}_{ie}^b) \end{pmatrix}, \qquad (2)$$

where $\boldsymbol{\Omega}_{ib}^b$ is the skew-symmetrical form of the angular velocity vector $\boldsymbol{\omega}_{ib}^b$ and the dot above a vector (bold lower case) or a matrix (bold capital) indicates differentiation. Note that the m-frame in the geo-referencing formula (1) has been replaced by the e-frame. This system is integrated to yield the parameters on the left-hand side, namely position, velocity, and the orthogonal rotation matrix $\mathbf{R}_b^e$ between the b-frame and the e-frame. The determination of this time-variable matrix is one of the central tasks of geo-referencing.

The integration of the system of differential equation is started by initializing the parameters on the left-hand side of the equation. Traditionally, this is done in stationary mode. In that case, the initial velocity is zero, the initial position is obtained from GPS, and the initial orientation matrix is determined by an alignment procedure that makes use of accelerometer leveling and gyro compassing. The alignment is usually done in two steps. In the coarse alignment simplified formulas are used to obtain pitch and roll from accelerometer measurements and azimuth from gyro measurements, within an accuracy of a few degrees. In the fine alignment small-angle error formulas are used in a filtering scheme to obtain more accurate estimates of the parameters. The rotation matrix $\mathbf{R}_b^e$ can then be obtained from the estimated pitch, roll, and azimuth or an equivalent parameterization, as for instance quaternions. This is the standard alignment procedure if sensor measurements from a navigation-grade inertial system are available. For medium and low accuracy systems, this method cannot be applied. Because of the unfavorable signal-to-noise ratio for $\boldsymbol{\omega}_{ib}^b$ the gyro compassing procedure will not converge. Thus, stationary alignment cannot be used with MEMS-based or other low-accuracy IMUs.

The alternative is in-motion alignment. This method has mainly been used in airborne applications, specifically for the in-air alignment of inertial systems. It is obviously dependent on using additional sensors, which in this case are GPS receiver outputs, i.e. position and/or velocity in the e-frame. In-motion alignment makes use of the fact that very accurate position information is available at a high data rate. It is therefore possible to determine accurate local-level velocities. By combining these velocities with the ones obtained from the strapdown IMU, the rotation matrix $\mathbf{R}_b^e$ can be determined.

When implementing this approach for medium or low accuracy IMUs two difficulties have to be addressed. The first one is that either no azimuth information at all is available, or that it is derived from GPS velocities and is rather inaccurate. Thus, the standard small-angle error models cannot be used any more because the azimuth error can be large. By reformulating the velocity error equations, one can arrive at a set of equations that converges quickly for azimuth, even if the initial errors are large. Scherzinger (1994) has given a thorough discussion of the problem and its solutions, based on earlier work by Benson (1975). A land vehicle application, using a MEMS-IMU integrated with GPS, is given in Shin and El-Sheimy (2004). Convergence is fast in this case, taking only about 50 s. This bodes well for airborne applications where, due to the higher velocities, a better signal-to-noise ratio should further improve the results.

The second difficulty is more fundamental. It has to do with the way in which the non-linearity in equation system (2) and in the corresponding GPS measurements are handled. The standard approach is to expand the errors in position, velocity, and orientation into a Taylor series and to truncate the series after the linear term. The error equations obtained in this way are then cast into state vector form. By adding the linearized GPS measurements to the model and by representing the state variable distribution by a Gaussian random variable, the

extended Kalman filter (EKF) can be formulated. It is a standard tool in engineering that is frequently used when either the system model or the observation model are non-linear. In an interesting paper Julier and Uhlmann (1996) have demonstrated that even in a seemingly innocuous situation - a road vehicle moving along a circle - the EKF does not handle the non-linearity in an acceptable manner. After a quarter circle, the covariance propagation results in error ellipses that do not represent the actual situation. The authors show quite convincingly that this is due to the linearized covariance propagation. To rectify the situation, the authors propose to change this part of the EKF. They approximate the Gaussian distribution at a carefully chosen set of points and propagate this information through the non-linear equations. In this way the transformed Gaussian distribution will reflect the non-linearities of the system better. The new filter, called the Unscented Kalman Filter (UKF) by its authors, has received some attention during the past few years, see for instance Julier and Uhlmann (2002) and Crassidis and Markley (2003). A paper that combines in-motion alignment, large azimuth modeling and UKF for MEMS /DGPS integration is Shin and El-Sheimy (2004). Although the UKF does not often show a substantial increase in accuracy, it seems to be more robust than the EKF in critical situations.

Another approach based on Neural Networks (NN) has been proposed by Chiang and El-Sheimy (2002). They suggested an INS/GPS integration algorithm utilizing multi-layer neural networks for fusing data from DGPS and either navigation grade IMUs or tactical grade IMUs. Artificial Neural Networks (ANNs) have been quite promising in offering alternative solutions to many engineering problems, where traditional models have failed or were too complicated to build. Due to the nonlinear nature of ANNs, they are able to express much more complex phenomena than some linear modeling techniques. They extract the essential characteristics from the numerical data as opposed to memorizing all of it. ANNs, therefore, offer a convenient way to form an implicit model without necessarily establishing a traditional, physical mathematical model of the underlying phenomenon (see Figure 6). In contrast to traditional Kalman Filtering models, ANNs require only a little or no a priori knowledge of the underlying mathematical process. For GPS/INS integration, this simply means that integration architecture is platform and system independent, as long as the implicit functional relationship between the input and output is fixed.

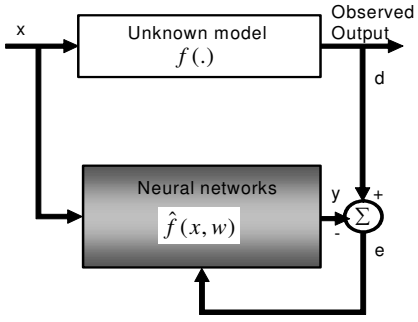

Figure 6: Supervised learning as model identification or function approximation

5. FILTERING AND SMOOTHING

The discussion in the last chapter indicated already that modeling and estimation are closely connected in the geo-referencing problem. In terms of interesting recent contributions in filtering and smoothing, three topics will be discussed: Denoising, AR modeling, and simplified smoothing. All three are post-mission methods and are well suited to mobile mapping. Denoising is an important aspect in post-mission IMU modeling because the noise level of inertial sensors is very high, typically 20 000 – 30 000 times higher than the minimum signal to be resolved. In real-time applications the standard way of treating this problem is to trust integration to work as a filter and to carefully select the white noise components in the Kalman filter. In mobile mapping where most applications are processed in post mission, denoising often allows a more refined analysis because the spectral band of interest can be defined and the high-noise band can be eliminated. This is of importance when one tries to model the bias terms in the Kalman filter, as in case of autoregressive modeling (AR). Without denoising the results of an AR analysis become meaningless. Post-mission processing has also the advantage that trajectory constraints can be applied in both forward and backward direction, while in real-time Kalman filtering this is only possible in forward direction. Since an optimal smoother is time consuming and requires considerable storage capacity, a simplified model for backward smoothing will also be briefly discussed.

Band limiting and denoising describes a variety of techniques that can be used to eliminate white or colored noise from observations. Skaloud et al (1999) were the first to apply wavelet denoising to the raw data from inertial sensors. They were able to show that the accuracy of the estimated orientation parameters improved by a factor of five, resulting in standard deviations of about 10 arcseconds for pitch and roll, and of 20 arcseconds for azimuth for a medium accuracy IMU. In Figure 7, the rather dramatic noise reduction is shown when applying a wavelet filter to a set of accelerometer measurements. The noise drops from a standard deviation of about 2 000 mGal (a) to about 10 mGal (b). Further work in this area was done by Noureldin et al (2002) who used forward linear prediction to design a tap delay line filter to improve the performance of a FOG gyro by eliminating the short-term angle random walk.

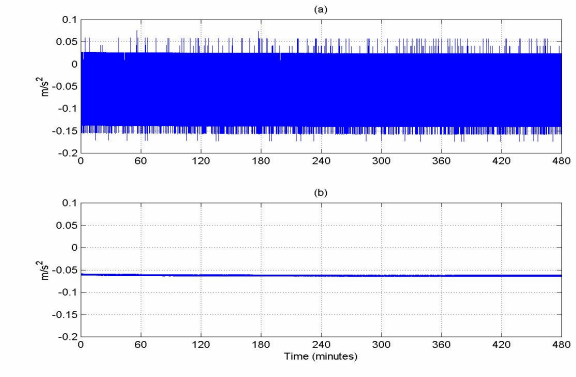

Figure 7: Y-Accelerometer Specific Force Measurements
(a) Before Wavelet De-noising
(b) After Applying the Wavelet 6th LOD

The state vector model typically used to process IMU data is made up of two sets of parameters. The first set contains the errors resulting from the Newtonian model, i.e. errors in position, velocity, and orientation. The second set contains the sensor errors, such as accelerometer and gyro biases. While the models for the first set of variables are given by the physics of the problem, the models for the second set are rather arbitrary. They are usually chosen by looking for a structure that makes state space modeling simple. Typical models of this type are random ramp, random walk, or first-order Gauss-Markov processes. Often a combination of these models is used to fit a specific error distribution, but in general model identification techniques are not applied to verify the model itself. Since most of the terms to be determined are long-wavelength features, an AR model can be used to determine what type of model structure would best fit the data. This idea was recently studied by Nassar et al (2003). Results are quite encouraging, especially if de-noising is applied first. The data sets studied so far all show significant second- order effects, and in some cases small third-order effects. When they are included in the state-space model, results improve by about 30%. However, if the order of the model is further increased, results get worse. Thus, it may be efficient and advisable to determine the optimal model order for typical classes of IMUs in advance and incorporate them into the state vector.

Post-mission processing, when compared to real-time filtering, has the advantage that data of the whole mission can be used to estimate the trajectory. This is not possible when using filtering because only part of the data is available at each trajectory point, except the last. When filtering has been used in a first step, one of the optimal smoothing methods, such as the Rauch et al (1965) algorithm can be applied. It uses the filtered results and their covariances as a first approximation. This approximation is improved by using the additional data that were not used in the filtering process. Depending on the type of data used, the improvement obtained by optimal smoothing can be considerable. This improvement comes at a price, however. The price is in terms of storage requirement and computation time. It is not only necessary to store all estimated state vectors, but also their complete covariance matrices before and after updates.

In cases where the IMU is mainly used to bridge GPS-outages, such as in land-vehicle applications in urban centers, a simple algorithm can be used very effectively. It calculates the difference between the IMU position and the GPS position at the beginning and the end of the outage. The resulting difference is attributed to a t^2-error. The choice of this simple error mode resulted from an analysis of the complete INS error model for short-time periods up to a few minutes; see Nassar and Schwarz (2002) for details. This model has been tested in both airborne and land-vehicle applications and has consistently modeled between 90%-95% of the accumulated error (ibid). Requirements in terms of storage and time are minimal and the algorithm is very simple. The error graph for a 85 second outage and its model fit is shown in Figure 8.

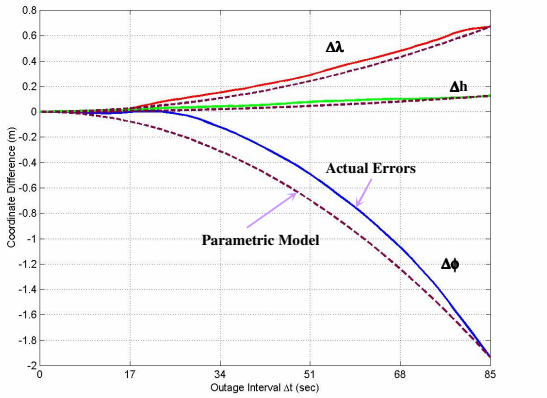

Figure 8: SINS (a navigation-grade - Honeywell LRF-III) Positioning Errors during DGPS Outage

6. CURRENTLY ACHIEVABLE ACCURACIES AND ONGOING DEVELOPMENTS

The tables of results shown in the following are not based on a comprehensive analysis of published results. They are rather samples of results achieved with specific imaging systems and have been taken from company brochures and technical publications. The authors think that they are representative for the systems that have been discussed previously. The following will include three examples of post-mission systems, one airborne, one van based, and one portable, and one airborne real-time system.

The accuracy specifications for the Applanix family of POS/AV™ airborne direct georeferencing systems are listed in Table 2 (Mostafa et al, 2000). The primary difference in system performance between the POS/AV™ 310 and POS/AV™ 510 systems is the orientation accuracy, which is directly a function of the IMU gyro drifts and noise characteristics. For example, the gyro drifts for the POS/AV™ 310 and POS/AV™ 510 systems are 0.5deg/h and 0.1deg/h, respectively. While the corresponding gyro noises are 0.15 and 0.02 deg/sqrt(h), respectively.

Parameter Accuracy (RMS)	POS/AV™ 210	POS/AV™ 310	POS/AV™ 410	POS/AV™ 510
Position (m)	0.05 - 0.30	0.05 - 0.30	0.05 - 0.30	0.05 - 0.30
Velocity (m/s)	0.010	0.010	0.005	0.005
Roll & Pitch (Deg)	0.040	0.013	0.008	0.005
True Heading (Deg)	0.080	0.035	0.015	0.008

Table 2: Post-processed POS/AV™ navigation parameter accuracy (Mostafa et al, 2000]

The second example is for land MMS. Accuracies achieved with many land MMS systems, such as the VISAT system (El-Sheimy, 1996) are suitable for all but the most demanding cadastral and engineering applications. Accuracies in this case mainly depend on availability of GPS and how long the INS systems can work independently in stand-alone mode. If GPS is available, the positioning accuracy is uniform at a level of 3-5 cm (rms). If GPS is not available, the positional accuracy depends on the length of the outage, see Table 3. It lists the stand-alone accuracy of a strapdown navigation-grade system

(iMAR® iNAV-RQH) from 30-180 seconds. These results have been obtained using the University of Calgary KINGSPADT^{M} GPS/INS integration software (www.kingspad.com). Further improvements in position and azimuth accuracy can be achieved if an odometer is added for length control and a two-antenna GPS for azimuth control. An interesting example on the use of a road vehicle in an extreme situation, the urban canyon environment of central Tokyo is given in Scherzinger (2002). Although adequate GPS coverage was denied for about 50% of the time, a position accuracy of better than25 cm was maintained for about 90% of the survey.

GPS Outags Periods	*KF (m)*	*Vehicle motion*
30 sec	***0.08***	*Straight line*
60 sec	***0.09***	*Circle*
30 Sec	***0.13***	*Curve*
60 Sec	***0.06***	*Static*
120 Sec	***0.12***	*Static*
180 Sec	***0.3***	*Straight line*

Table 3: Accuracy of the iMAR® iNAV-RQH INS system in stand-alone mode.

The third example given here is a backpack MMS developed at the University of Calgary. The backpack MMS competes in both accuracy and initial cost with current methods of GIS data collection, while offering increases in data collection efficiency and flexibility that only an MMS can provide. The backpack MMS uses a Leica Digital Magnetic Compass (DMC) for attitude determination, a single Kodak DC260, and a Novatel OEM4 receiver. The system's operational steps are essentially the same as any MMS in the sense that the DMC and the GPS provides the direct georeferencing information for the cameras. The only difference is that because of the low accuracy of the DMC derived attitude, the system is augmented with a Bundle Adjustment software, see Ellum (2001). In this case, the direct georeferencing parameters are used as apriori information on the exterior orientation parameters. The absolute accuracies of the Backpack MMS in a variety of configurations are shown Table 4. From the tables, it can be seen that with as few as five image point measurements at a 20m camera-to-object distance it is possible to achieve accuracies that satisfy many mapping applications, for more details see ibid.

The systems presented so far are working in post-mission mode of operation. In this mode of operation, the data is collected in the vehicle (van, airplane, or ship) and processed off-site in order to extract the information of interest. Due to the post-mission mode of operation, very high accuracy, in position (≤ 0.1 m "RMSE") and attitude (≈ 0.02 degrees "RMSE") can be achieved. This is accomplished by using the precise GPS carrier phase in Differential mode *(DGPS uses two GPS receivers; one in static mode over known control point and the second on the vehicle.* By tightly coupling DGPS and INS data through Kalman filtering the above accuracies can be achieved.

Number of Image Point	**Horizontal**		**Vertical**	
	Max (m)	*RMS (m)*	*Max (m)*	*RMS (m)*
3 Images				
5 Image Points	0.13	0.10	0.10	0.06
10 Image Points	0.13	0.10	0.12	0.07
6 Images				
5 Image Points	0.06	0.05	0.14	0.11
10 Image Points	0.07	0.05	0.17	0.11

Table 4: Backpack MMS System Absolute Accuracy (20m camera-to-object distance)

Although in most remote sensing applications, there is no need for real-time processing of the data, there are some emerging applications, specifically forest fire fighting; in which the requirement for real-time mapping is more important than the achievement of highest possible accuracy. One of the main problems in combating forest fires is monitoring the time history of the fire. Understanding the size, location, and speed of advance of the fire front is critical to the optimal allocation of fire-fighting resources and the maintenance of the fire crew safety. Investigations of major wild-land fire accidents involving loss of life, often indicate that the crews became imperiled because of insufficient or untimely information about the location and speed of the fire advance.

The F^3 system, being developed at the U of C, integrates imaging sensors (Thermal InfraRed "TIR" Cameras) with real time navigation technologies (Wide Area Differential GPS "WADGPS" and low cost INS). The system is very useful in reporting the exact situation of fires, assisting the Forest Fire Information Systems (FFIS) in accurately assessing the fire and precisely directing water-bombers and fire-fighting crews. The use of infrared/thermal cameras, which sense the heat emitted in the form of infrared radiation, will enable early detection and location of forest fires in reduced visibility due to haze, smoke or darkness. Recent system testing over controlled fire pits of known coordinates indicates that the system's real-time positional accuracy in identifying hotspots is about 6m RMS (Wright and El-Sheimy, 2003), when using single receiver pseudo-ranges..

Kinematic GPS controlled aerial photogrammetry and direct geo-referencing using DGPS/INS have become mature technologies in both the scientific and commercial mapping communities. Virtually all airborne mapping systems now integrate a GPS receiver and INS unit with their camera. Unfortunately, on the software side, the integration of GPS or GPS/INS and photogrammetry is not as close. Typically, the GPS data is included in the photogrammetric bundle adjustment as processed positions only (Schmitz et al, 2001; Mikhail et al., 2001) and similarly the GPS/INS data are used for direct georeferencing. In effect, the processing engines of GPS (or GPS/INS) and photogrammetry operate largely in isolation. This implementation has obvious benefits in terms of simplicity. However, a more fundamental fusion of the GPS and INS data

into the bundle adjustment may provide improvements in both accuracy and reliability. A tighter coupling of the GPS and photogrammetric processing engines where the GPS code pseudoranges are directly included in the bundle adjustment is currently investigated at the university of Calgary [Ellum, 2004]. The goal of this integration is to improve the accuracy and reliability when compared to the simple inclusion of GPS positions. It is hoped that accuracies similar to those obtained by a wide-area augmentation system can be achieved.

A more far-reaching step would the development of two-way information sharing between a photogrammetric adjustment and the kinematic GPS/INS processing. In this architecture, a Kalman-filter-based kinematic GPS/INS processor provides precise position and orientation to the photogrammetric adjustment. In turn, the photogrammetric adjustment provides position updates to the Kalman filter. These position updates should aid the ambiguity resolution of the GPS/INS processor, making the entire process more accurate and more robust. This will be of major importance to mobile mapping with land vehicles, as it will result in a more consistent mapping space accuracy. This will reduce the requirement for zero-velocity updates (ZUPTS), when signal outages occur (i.e., bridging), and will allow to reinitialize the GPS ambiguities to integer values following outages.

7. CONCLUSIONS

T Looking at the development of Mobile Mapping Systems over the past fifteen years the following conclusions can be drawn:

- Mobile mapping, the combination of digital imaging and geo-referencing, has developed from a topic of academic interest to a commercially viable industry with airborne, land-based, and marine applications.
- With the still rapid development of high-resolution digital frame cameras and the current testing of digital scanners that promise higher resolution than film-based cameras, economy and efficiency are on the side of this new technology.
- The geo-referencing technology has matured, due to the ongoing refinement and miniaturization of GPS-receiver hardware and the use of low and medium cost IMU's, and has become more affordable during the past decade. It appears that a major step forward is imminent as MEMS sensor technology will result in considerable cost reductions for tactical-grade gyros and in new multi-sensor system concepts.
- The ongoing development of mathematical modeling and advanced post-mission estimation techniques will further increase accuracy and robustness of the solutions.

Furthermore, some emerging real-time problems may have considerable socio-economic impact in applications such as fire fighting or offshore pollution control.

8. REFERENCES

Bader, J. (1993): Low-Cost GPS/INS. Proc. ION GPS-93, Salt Lake City, USA, pp. 135 - 244

Bäumker, M. and A. Mattissek (1992): Integration of a Fibre Optical Gyro Attitude and Heading Reference System with Differential GPS. Proc. ION GPS-92, Albuquerque, USA, Sept. 16 – 18, 1992, pp. 1093 – 1101.

Benson Jr, D.O. (1975): A Comparison of Two Approaches to Pure-inertial and Doppler-inertial Error Analysis. IEEE Transactions on Aerospace and Electronic Systems, Vol. AES-11, No 4, July 1975.

Cannon, M.E. and K.P. Schwarz (1990): A Discussion of GPS/INS Integration for Photogrammetric Applications. Proc. IAG Symp. # 107: Kinematic Systems in Geodesy, Surveying and Remote Sensing, Banff, Sept. 10-13, 1990, pp. 443-452 (published by Springer Verlag), New York

Chiang, K.W. and El-Sheimy, N. (2002): INS/GPS Integration using Neural Networks for Land Vehicle Navigation Applications, Proceedings of the US Institute of Navigation (ION) GPS'2002 meeting, September 24-27, 2002 - Oregon Convention Center, Portland, Oregon, USA (CD).

Cosandier, D., M.A. Chapman, T. Ivanco (1993): Low Cost Attitude Systems for Airborne Remote Sensing and Photogrammetry. Proc. of GIS93 Conference, Ottawa, March 1993, pp. 295-303.

Crassidis, J.J. and F.L. Markley (2003): Unscented Filtering for Spacecraft Attitude Estimation. J. of Guidance, Control, and Dynamics, July/Aug. 2003, Vol. 26, No. 4, pp 536 – 542.

Doerstel,C., Zeitler, W., Jacobsen, K., 2002: Geometric Calibration of the DMC: Method and Results, ISPRS Com I and PECORA, Denver 2002

Ellum, C. (2004): Integration of Raw GPS Measurements into a Bundle Adjustment. In XX ISPRS Congress, International Archives of Photogrammetry and Remote Sensing, International Society of Photogrammetry and Remote Sensing (ISPRS), Istanbul, accepted for publication.

Ellum, C (2001), The Development of a Backpack Mobile Mapping System, (M.Sc. thesis), UCGE Report No. 20159, Department of Geomatics Engineering, the University of Calgary.

El-Sheimy, N. and K.P. Schwarz (1993): Kinematic Positioning in Three Dimensions Using CCD Technology. Proc. IEEE/IEE Vehicle Navigation & Information System Conference (IVHS), October 12-15, 1993, pp. 472-475.

El-Sheimy, N (1996), The Development of VISAT - A Mobile Survey System for GIS Applications, (Ph.D. thesis), UCGE Report No. 20101, Department of Geomatics Engineering, the University of Calgary.

Geen, J.A. (2004): Progress in Integrated Gyroscopes. Proc. IEEE PLANS 2004, Monterey, USA, April 26-29, 2004, pp. 1 – 6.

Hanse, J.G (2004): Honeywell MEMS Inertial Technology & Product Status. Proc. IEEE PLANS 2004, Monterey, USA, April 26-29, 2004, pp. 43 - 48.

Julier, S.J. and J.K. Uhlmann (1996): A General Approach for Approximating Nonlinear Transformations of probability Distributions. Technical Report, Department of Engineering Science, University of Oxford, UK.

Julier, S.J. and J.K. Uhlmann (2002): The Scaled Unscented Transformation. Proc. IEEE American Control Conference, Anchorage, USA, 2002, pp.4555 ñ 4559.

Lapucha, D., K.P. Schwarz, M.E. Cannon, H. Martell (1990): The Use of GPS/INS in a Kinematic Survey System, Proc. IEEE PLANS 1990, Las Vegas, March 20-23, 1990, pp. 413 – 420.

Lipman J.S. (1992): Trade-Offs in the Implementation of Integrated GPS Inertial Systems. Proc. ION GPS-92, Albuquerque, USA, Sept. 16 – 18, 1992, pp. 1125 – 1133.

Mikhail, E. M., J. S. Bethel, and J. C. McGlone, 2001, Introduction to Modern Photogrammetry. John Wiley and Sons, Inc., New York.

Mostafa, M.M.R. and K.P. Schwarz (2000): A Multi-Sensor System for Airborne Image Capture and Georeferencing. PE&RS, Vol. 66, No. 12, pp. 1417 – 1424.

Mohamed Mostafa, Joe Hutton, Erik Lithopoulos (2000a): Ground Accuracy from Directly Georeferenced Imagery, GIM International Vol. 14, No. 12, pp.

Mostafa, M. (2004): The Digital Sensor System Data Flow, The 4th International Symposium on Mobile Mapping Technology, Kunming, China, April 2004 (CD).

Nassar, S. and K.P. Schwarz (2002): Bridging DGPS Outages in Kinematic Applications Using a Simple Algorithm for INS Bias Modeling. Proc. ION GPS-2002, Portland, USA, Sept. 24-27, 2002, pp. 1474 – 1482.

Nassar, S., K.P. Schwarz, A. Noureldin, N. El-Sheimy (2003): Modeling Inertial Sensor Errors Using Autoregressive (AR) Models. Proc. ION NTM-2003, Anaheim, USA, January 22-24, 2003, pp.116-125.

Noureldin, A., D. Irvine Halliday, H. tabler, M.P. Mintchev (2002): New Technique for Reducing the angle random walk at the Output of Fibre Optic Gyroscopes During Alignment Processes of Inertial Navigation Systems. Opt. Eng. Vol. 40, No. 10, pp. 2097 – 2106 (October 2001).

Novak, K. 1993. Data collection for multi-media GIS using mobile mapping systems. Geomatics Info Magazine (GIM). Vol. 7. No. 3. pp. 30-32.

H.E. Rauch, F. Tung, C.T. Striebel (1965): Maximum Likelihood Estimates of Linear Dynamic Systems, AIAA J., Vol. 3, No.8, pp. 1445 - 1450.

Scherzinger, B.M. (1994): Inertial Navigator Error Models for Large Heading Uncertainty. Proc. Int. Symp. Kinematic Systems in Geodesy, Geomatics and Navigation, Banff, Canada, Aug. 30- Sept. 2, 1994, pp. 121-130.

Scherzinger, B.M. (2002): Inertially Aided RTK Performance Evaluation. Proc. ION GPS-2002, Portland, USA, Sept. 24-27, 2002, pp. 1429 ñ 1433.

Schmitz, M., G. W¨ubbena, and A. Bagge, 2001, Benefit of Rigorous Modeling of GPS in Combined AT/GPS/IMU-Bundle Block Adjustment. In OEEPE Workshop on Integrated Sensor Orientation, Organisation Europene d'Etudes Photogrammtriques Exprimentales/ European Organization for Experimental Photogrammetric Research (OEEPE), Hannover.

Schwarz, K.P., M.A. Chapman, M.E. Cannon, P. Gong (1993): An Integrated INS/GPS Approach to the Georeferencing of Remotely Sensed Data. PE&RS, Vol. 59, No. 11, pp. 1667-1674.

Schwarz, K.P. (2000): Mapping the Earth's Surface and Its Gravity Field by Integrated Kinematic Systems. Lecture Notes of the Nordic Autumn School, Fevic, Norway, Aug. 28 – Sept. 1, 2000, pp.

Shin, E.H. and N. El-Sheimy (2003): INS Toolbox, a MatLab software for GPS/INS integration, Department of Geomatics Engineering, the University of Calgary (http://www.geomatics.ucalgary.ca/research/MMSensor/facilities/software/instoolboxformatLab.php)

Shin, E.H. and N. El-Sheimy (2004): An Unscented Kalman Filter for In-Motion Alignment of Low-Cost IMU's, IEEE PLANS 2004 APRIL 26- 29, 2004 - MONTEREY, CA, pp 273 - 279.

Skaloud, J., A.M. Bruton, K.P. Schwarz (1999): Detection and Filtering of Short-term (1/f) Noise in Inertial Sensors. Navigation, Journal of The Institute of Navigation, Vol. 46. No. 2. pp. 97-107.

Wright, B. and El-Sheimy, N. (2003): "Real-Time Direct Georeferencing of Thermal Images For Identification and Location of Forest Fire Hotspots", 6th Conference on Optical 3D Measurement Techniques, Zurich, Switzerland, September 22-25, 2003 (CD).